ChemComm

ROYAL SOCIETY OF CHEMISTRY

COMMUNICATION

View Article Online
View Journal | View Issue

Cite this: *Chem. Commun.*, 2022, **58**, 439

Received 31st October 2021,
Accepted 30th November 2021

DOI: 10.1039/d1cc06147j

rsc.li/chemcomm

Non-invasive, 3D printed, colourimetric, early wound-infection indicator†

Dilidaer Yusufu,[a] Erin Magee,[b] Brendan Gilmore[b] and Andrew Mills *[a]

A simple, non-invasive, colour-based carbon dioxide (CO_2) indicator is described. The indicator provides an indirect response to the rapid, aerobic microbial colonisation of an underlying wound when used in conjunction with an occlusive (*i.e.* sealed) dressing. The indicator has potential as an early warning indicator of infection in chronic wounds.

Chronic wounds can be defined as ones that do not heal within 3 months[1] and so are particularly vulnerable to infection and require careful tending and continuous monitoring, which is costly. It is estimated that in the UK alone the annual cost of managing chronic wounds is over £3.2 billion[2] and this figure continues to increase as the average age of the population increases.[3]

As illustrated by the schematic in Fig. 1, the main stages of the wound infection continuum are contamination, colonisation, local infection, spreading infection and systemic infection, with local infection characterised initially by covert and then overt signs of infection. As indicated in Fig. 1, the start of infection is often accompanied by the start of biofilm formation.[4]

The assessment of the condition of a chronic wound is usually made when its dressing is changed, the regularity of which depends upon the nature and state of the wound, but typically is every few days. Wound assessment is often subjective, as it is made by the patient and/or healthcare professional *via* the recognition of local overt signs of infection, such as a rise in temperature, erythema, swelling and/or a purulent discharge,[4] or non-specific general signs (such as loss of appetite or energy).[5] Note, however, by the time such indicators of infection appear, the infection has often taken hold and rapid intervention is required.

The microflora associated with infected wounds often comprise similar levels of aerobes and anaerobes.[3] The link between the density of aerobic and anaerobic microorganisms, *i.e.* microbial load, and infection is still the subject of much debate.[3,6] However, many believe that microbial load is a critical factor in determining whether a wound is likely to heal or not. This view is supported by the results of numerous studies, such as those of Bendy *et al.*, who found that healing of pressure ulcers was only possible when the aerobic microbial load was $<10^6$ colony forming units (CFU) per mL of wound fluid.[7] Others have reported a similar critical load value per g of tissue.[8] Thus, it seems highly desirable that the microbial load associated with a wound is measured regularly during treatment. However, even the measurement of aerobic microbial load, which is easier than that for anaerobes, is relatively expensive, time-consuming, and has the potential to cause further trauma and create routes to infection. As a consequence, such measurements are rarely made in the management of chronic wounds,[1] and monitoring is largely restricted to looking for signs and symptoms of infection. Not surprisingly, a number of smart wound dressings capable of reporting early stages of microbial growth through biological indicators such as uric acid, pH, oxygen, bacteria and temperature, have been developed.[9,10] Table S1 in Section S1 of the ESI† file lists some examples of such dressings.

Concerns regarding wound infection have resulted in an increasing use of occlusive (*i.e.* sealed) dressings, especially since research shows that the infection rate is lower with

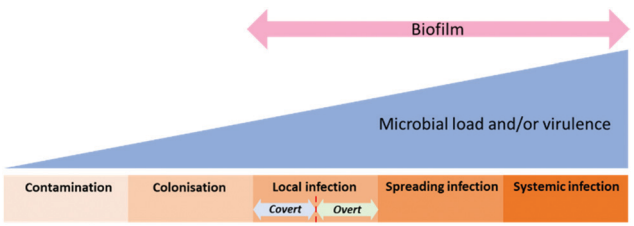

Fig. 1 Schematic illustration of the wound-infection continuum.[4]

[a] *School of Chemistry and Chemical Engineering, Queens University Belfast, David Keir Building, Stranmillis Road, Belfast, BT9 5AG, UK. E-mail: andrew.mills@qub.ac.uk*
[b] *School of Pharmacy, Queen's University Belfast, Belfast, BT9 7BL, UK*

† Electronic supplementary information (ESI) available. See DOI: 10.1039/d1cc06147j

occlusive rather than conventional dry dressings and wound healing is not hindered.[11] As their name suggests, occlusive dressings seal the wound and its surrounding tissue off from the *ambient air*, fluids, and harmful contaminants, such as viruses and bacteria. It follows that for all wounds with an occlusive dressing, there exists a headspace between the wound and the outer thin plastic film, usually polyurethane, of the dressing, that is different from that of ambient air and reflects to some extent the microbial condition of the wound. The existence of this headspace presents a sensing opportunity since its composition is likely to change markedly if the wound becomes contaminated with one or more aerobic microbiological species and significant, rapid colonisation, leading to infection, occurs. Most obviously, if the wound's aerobic microbial load increases markedly, so will the level of aerobic microbial metabolism, which will be reflected by a marked increase in the $\%CO_2$ in the headspace from the initial ambient level of *ca.* 0.04% associated with air.

In this communication, we report on the use of a simple, inexpensive, 3D printed, colourimetric CO_2 indicator for monitoring the headspace above an infected wound model, based on an inoculated *ex vivo* porcine-skin sample,[12] covered with a common commercial occlusive wound dressing. A schematic illustration of the overall system used in this work is illustrated in Fig. 2. The transparent nature of the dressing allows the indicator to be monitored qualitatively by eye or quantitatively using digital photography coupled with digital colour analysis, *i.e.* DCA,[13] which may be provided by a mobile phone camera with a colour-analysis App, for example. The indicator is non-invasive since it monitors only the headspace and there is no contact between the indicator and the wound.

Colourimetric CO_2 indicators represent a well-established technology based on the protonation of a pH-sensitive anionic dye, D^-, to DH, by carbonic acid, H_2CO_3, derived from the CO_2 in the ambient atmosphere. Most current CO_2 colourimetric indicators are made using solvent-based inks, in which D^- is ion-paired with a quaternary cation, Q^+, to form a product, $Q^+D^-{\cdot}xH_2O$, that is soluble in the hydrophobic polymer/resin in the ink.[14] Once cast as a film and allowed to dry, the $Q^+D^-{\cdot}xH_2O$/polymer ink film exhibits a reversible response due to the following equilibrium reaction,

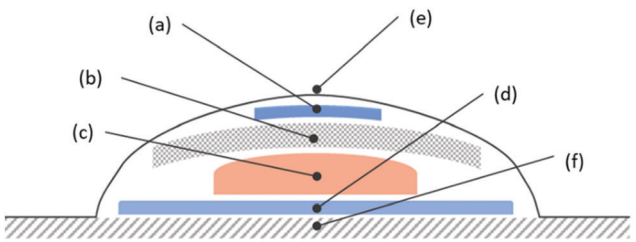

Fig. 2 Schematic illustration of the (a) 3D printed, colourimetric, CO_2 plastic film indicator, (b) lint dressing, (c) inoculated *ex vivo* porcine-skin sample system on a (d) damped absorbent pad, covered with a (e) clear, commercial occlusive wound dressing, and sealed onto a (f) support substrate of polyethylene terephthalate (PET).

$$Q^+D^-{\cdot}xH_2O + CO_2 \rightleftharpoons Q^+HCO_3^-{\cdot}(x-1)H_2O{\cdot}HD \quad (1)$$

where $Q^+D^-{\cdot}xH_2O$ and $Q^+HCO_3^-{\cdot}(x-1)H_2O{\cdot}HD$ are the lipophilic equivalent versions of the very differently coloured deprotonated and protonated forms of the dye in aqueous solution, *i.e.* D^- and DH, respectively. Work shows that the sensitivity of the CO_2 indicator can be varied, *i.e.* tuned, by using different pH-indicating dyes with different pK_a values; the greater the pK_a, the greater the sensitivity of the CO_2 indicator.[15] Most current commercial CO_2 indicators are used to monitor CO_2 levels in food packages (where $\%CO_2 > 40\%$) and so employ dyes, such as phenol red ($pK_a = 7.52$),[15] that produce indicators with an appropriately low sensitivity.[16] In contrast, the CO_2 indicator for monitoring a wound needs to be much more sensitive and so must employ a dye with a much larger pK_a. In this work xylenol blue, XB, was used for this purpose, as it has a $pK_a = 9.52$.

The absorbance of the CO_2 indicator, $A(D^-)$, can be related to the $\%CO_2$ in the atmosphere surrounding the indicator using eqn (1). Recent work has established that the photographic image of such an indicator, coupled with DCA based on the red (R), green (G) and blue (B), *i.e.* RGB, components of the image, can be used to yield a value for the apparent absorbance, A', of the indicator that is directly proportional to $A(D^-)$. For a blue coloured dye, such as used in this work,

$$A' = \log\{255/\mathrm{RGB(red)}\} \quad (2)$$

where RGB(red) is the value of the red parameter in the RGB-analysed image of the indicator.[13]

Recently, this group has incorporated colourimetric CO_2 inks into extruded plastics films using a CO_2 sensitive pigment, generated by coating the ink onto silica pigment particles.[17] In this communication, we have taken this one step further and, for the first time, 3D printed the CO_2 indicator, as it is an ideal method for the low cost scaled up production of plastic materials. Full experimental details associated with the work described here, including how the indicators were made, are given in section S2 of the ESI.† Section S3 in the ESI† describes the results of a study of the XB indicator as a CO_2 indicator, which are summarised briefly as follows. The indicator is blue in the absence of CO_2 and bright yellow in its presence and responds reversibly to CO_2. The indicator exhibits a 50% overall colour change response time of *ca.* 0.2 min (air to 100% CO_2) and a recovery time of 8 min (100% CO_2 to air). The indicator exhibits a halfway change in its colour (*i.e.* when it was green) at *ca.* 1.3% CO_2 at 30 °C, which was the incubation temperature used when testing the indicator in the dressed, simulated wound system illustrated in Fig. 2.

A well-established, *ex vivo* porcine skin infected wound model was used to test the efficacy of the CO_2 indicator[12] in the dressed simulated wound system illustrated in Fig. 2. In this work, depilated, 14 mm diameter piglet skin samples were scored in a criss-cross fashion using a surgical scalpel to create a wound bed. These samples were then uniformly inoculated with a 20 μL aqueous dispersion of the microbial species under test, usually the common wound pathogen *Pseudomonas*

aeruginosa (*P. aeruginosa*),[3] the load of which was varied from 10^3 to 10^8 CFU mL^{-1}. Each inoculated pig skin sample was then used in the dressed, simulated wound system illustrated in Fig. 2, incubated at 30 °C. The colour of the indicator in the dressing was recorded hourly as a function of time using digital photography and the results of this work are illustrated in Fig. 3(a). Note that whilst most of the samples were inoculated with different, known levels of *P. aeruginosa*, the two exceptions were the control samples, C1, which had a wound bed that was not inoculated with *P. aeruginosa*, and C2, which had no wound bed, *i.e.* used undamaged skin, but was inoculated with 10^6 CFU mL^{-1} of *P. aeruginosa*.

A brief inspection of the photographs illustrated in Fig. 3(a) reveals that the CO_2 indicator in the C1 and C2 samples did not change colour over the 24 h incubation period, thereby indicating no significant CO_2 production. These results suggest that no marked, rapid colonisation of the *P. aeruginosa* occurs for these two control samples. In sharp contrast, the photographs in Fig. 3(a) also show that when the wound bed was inoculated with *P. aeruginosa*, the CO_2 indicator turned yellow, thereby indicating a significant level, *i.e.* > *ca.* 3%, of CO_2 in the headspace of the wound dressing, after an incubation time that decreased with increasing CFU mL^{-1} inoculum load. Subsequent, digital colour analysis of the photographs in Fig. 3(a) yielded the series of plots of apparent absorbance, A', *vs.* incubation time illustrated in Fig. 3(b), which helps identify, for each different inoculum, the time taken for the CO_2 indicator to change from its initial blue colour to yellow, at which point the CO_2 level in the headspace of wound dressing exceeds *ca.* 3.0%. In this work the incubation time at which the apparent absorbance of each CO_2 indicator reached *ca.* 0.6, *i.e.* $t(A' = 0.6)$ when the indicator was halfway through its colour transition and green, is identified for each different inoculum by a vertical red line.

In a separate set of otherwise identical experiments to those used to generate the data in Fig. 3, the value of the total microbial load (units: CFU per g of tissue) on each sample of the inoculated wounded pig skin was measured at 0, 6, 12 and 24 h incubation times and the results of this work are illustrated in Fig. 4(a). These results show that, for all the inoculated samples, the microbial load increased with increasing incubation time until, for most samples, a maximum value of *ca.* 10^9 CFU per g of tissue was reached. Where possible, for each of the log CFU g^{-1} *vs.* incubation time profiles illustrated in Fig. 4(a), the time taken to reach a value of 10^6 CFU g^{-1}, *i.e.* $t(10^6)$, was determined and is highlighted in the plot by a vertical red line. Interestingly, the subsequent plot of $t(A' = 0.6)$ *vs.* $t(10^6)$, illustrated in Fig. 4(b), reveals a good straight line, which suggests that the (incubation) time taken for the CO_2 indicator to reach an absorbance of *ca.* 0.6, at which point it has changed from blue to green, is directly related to the time taken to reach what many believe is a critical aerobic microbial load, sometimes referred to as critical colonisation threshold, *i.e.* CCT,[18] of *ca.* 10^6 CFU g^{-1} of *P. aeruginosa*. The non-zero intercept is a reminder that when the initial inoculum is $>10^6$ CFU g^{-1}, the CO_2 indicator will not respond immediately as it requires the microbes to respire for sufficient time for

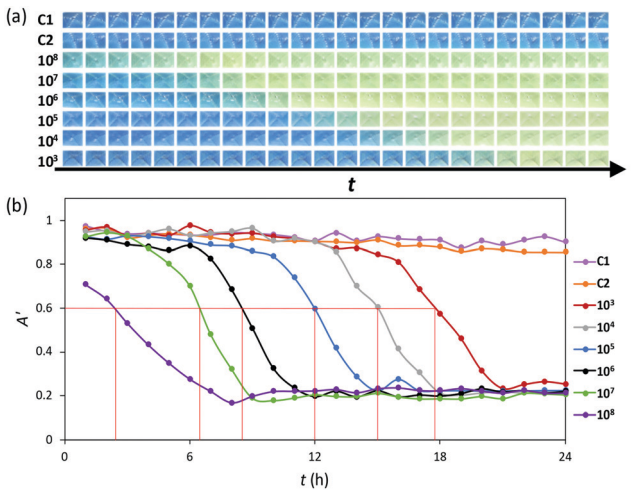

Fig. 3 (a) Photographic images of the 3D printed XB CO_2 indicator in the dressed, inoculated wound illustrated in Fig. 2 recorded as a function of incubation time, *t*, at 30 °C, every hour for 24 h, with initial inoculums of 10^3–10^8 CFU mL^{-1} of *P. aeruginosa*. The C1 and C2 images are for control samples where the porcine skin was either not inoculated, or not scored (but inoculated with 10^6 CFU mL^{-1} of *P. aeruginosa*), respectively. (b) Plots of apparent absorbance of the indicator film, *i.e.* A', as a function *t*, calculated using eqn (2) and data derived from the digital images illustrated in (a). The initial inoculums used spanned the range 10^3–10^8 of CFU mL^{-1} of *P. aeruginosa*. The two horizontal lines were derived from the same analysis carried out as before but this time using the images recorded for the C1 and C2 samples.

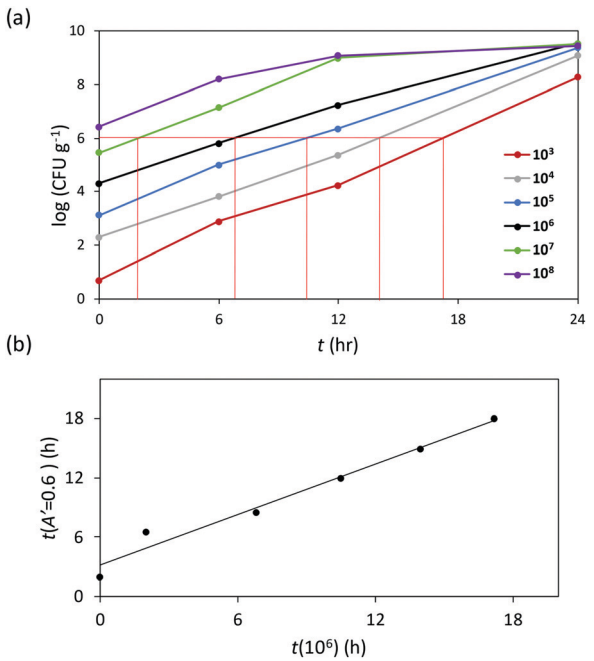

Fig. 4 (a) Plot of measured log(CFU g^{-1}) of *P. aeruginosa* as a function of incubation time, *t*, for an identical set of dressed, inoculated porcine skin wound samples as used to generate the data in Fig. 3; thus, with samples incubated at 30 °C, with initial inoculums ranging from 10^3–10^8 CFU mL^{-1}. (b) Plot of $t(A' = 0.6)$ – from Fig. 3(b) – *vs.* $t(10^6)$ – from (a).

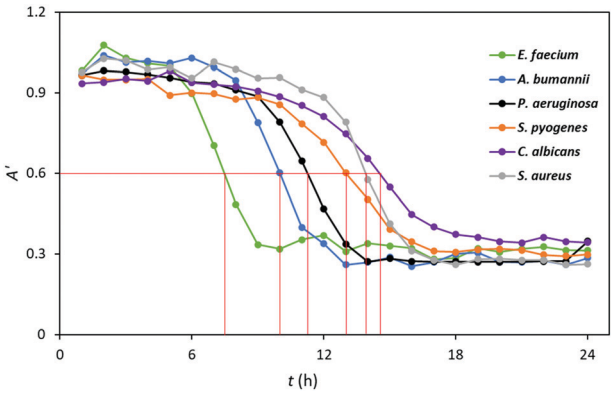

Fig. 5 Plots of apparent absorbance of the indicator film, *i.e.* A', calculated using eqn (2), as a function incubation time, t, for dressed wounded, porcine skin inoculated with 20 μL loaded 10^5 CFU mL^{-1} of a range of different microbial species. These plots were generated using DCA data derived from the digital images illustrated in Fig. S5.1 in the ESI.†

the %CO_2 level in the headspace to exceed *ca.* 3%. The linear correlation between $t(A' = 0.6)$ and $t(10^6)$, illustrated in Fig. 4(b), is not too surprising, given the otherwise identical, and therefore unrealistic, nature of the dressed samples. However, in relation to real wounds the above results suggest that the CO_2 indicator could be used to provide a clear indication of the rapid aerobic microbial growth and associated increase in microbial load that usually is a precursor to infection.

The wound infection continuum illustrated in Fig. 1, indicates that often biofilm formation is closely associated with the microbial load exceeding the CCT and infection taking hold. Although, a significant rise in CO_2 does not necessarily signify biofilm formation, *P. aeruginosa* is a well-known biofilm former, and the eventual formation and subsequent growth of a biofilm after an incubation time of *ca.* 12 h was confirmed using wounded pig skin samples inoculated with 20 μL loaded 10^6 CFU mL^{-1} of *P. aeruginosa*, as illustrated by Fig. S4.1 in Section S4 in the ESI.† Although biofilm formation appears to start at *ca.* 12 h, from the results illustrated in Fig. 3 and 4 it appears the same inoculum produces values of $t(A' = 0.6)$ and $t(10^6)$ of *ca.* 7 h, which shows that, in the case of *P. aeruginosa*, the CO_2 indicator is able to signal the rapid microbial colonization of the wound, and approach to the CCT, *before* biofilm formation and infection.

Most wounds are colonized by multiple bacterial species, but at sufficiently low levels that they do not inhibit the healing process, *i.e.* well below the CCT.[18] It is important, therefore, to demonstrate that the CO_2 indicator works with wound infection microbial species other than *P. aeruginosa*. Thus, in another set of experiments using the same system as illustrated in Fig. 2, the porcine skin wound was inoculated with 20 μL of 10^5 CFU mL^{-1} of each of the following wound pathogenic species, *E. faecium, A. baumannii, S. pyogenes, C. albicans, and S. aureus*, with *P. aeruginosa* for comparison purposes. The resulting photographs of the CO_2 indicator as a function of incubation time are illustrated in Fig. S5.1 in Section S5 the ESI,† from which the plots of apparent absorbance of the indicator film, A', as a function of incubation time, t, illustrated in Fig. 5 were generated.

Not surprisingly the results in Fig. 5 show that different aerobic pathogens grow at different rates, with *E. faecium* the fastest and *C. albicans*, the slowest. As before, a similar set of experiments were carried out in which the microbial load was monitored as a function of incubation time and the results are illustrated in Fig. S5.3 in Section S5 in the ESI.† Using the data in Fig. 5 and that in Fig. S5.3 in Section S5 in the ESI,† a plot of $t(A' = 0.6)$ *vs.* $t(10^6)$, illustrated in Figure S5.4 in Section S5 in the ESI,† was constructed to reveal a good straight line. These results show that, regardless of the aerobic microbial species used in this work, the CO_2 indicator appears to provide a good indication as to when the microbial load reaches *ca.* 10^6 CFU g^{-1}, since it is about the same time it takes for the indicator to reach an apparent absorbance of *ca.* 0.6. However, as noted earlier, the real value of the indicator is its ability to signal the onset of rapid aerobic microbial growth, through a striking blue to yellow colour change, which is likely to accompany the approach to the CCT and infection by aerobes. As such, the indicator has potential as an early warning wound-infection indicator.

Conflicts of interest

There are no conflicts to declare.

Notes and references

1 A. R. Siddiqui and J. M. Bernstein, *Clin. Dermatol.*, 2010, **28**, 519–526.
2 J. Guest, K. Vowden and P. Vowden, *J. Wound Care*, 2017, **26**, 292–303.
3 P. Bowler, B. Duerden and D. G. Armstrong, *Clin. Microbiol. Rev.*, 2001, **14**, 244–269.
4 E. Haesler and K. Ousey, *Wounds Int.*, 2018, **9**, 6–10.
5 A. McLister, J. McHugh, J. Cundell and J. Davis, *Adv. Mater.*, 2016, **28**, 5732–5737.
6 M. C. Robson, *Wound Repair Regen.*, 1999, **7**, 2–6.
7 R. Bendy, *Antimicrob. Agents Chemother.*, 1964, **4**, 147–155.
8 A. Kingsley, *Ostomy Wound Manage.*, 2003, **49**, 1–7.
9 E. Gianino, C. Miller and J. Gilmore, *Bioengineering*, 2018, **5**, 51.
10 M. Farahani and A. Shafiee, *Adv. Healthcare Mater.*, 2021, **10**, 2100477.
11 S. B. Rheinecker, *J. Athl. Train.*, 1995, **30**, 143.
12 Q. Yang, P. L. Phillips, E. M. Sampson, A. Progulske-Fox, S. Jin, P. Antonelli and G. S. Schultz, *Wound Repair Regen.*, 2013, **21**, 704–714.
13 D. Yusufu and A. Mills, *Sens. Actuators, B*, 2018, **273**, 1187–1194.
14 A. Mills and K. Eaton, *Quim. Anal.*, 2000, **19**, 75–86.
15 A. Mills and Q. Chang, *Anal. Chim. Acta*, 1994, **285**, 113–123.
16 D. Yusufu, C. Wang and A. Mills, *Food Packag. Shelf Life*, 2018, **17**, 107–113.
17 A. Mills and D. Yusufu, *Sens. Actuators, B*, 2016, **237**, 1076–1084.
18 N. Thet, D. Alves, J. Bean, S. Booth, J. Nzakizwanayo, A. Young, B. V. Jones and A. T. A. Jenkins, *ACS Appl. Mater. Interfaces*, 2016, **8**, 14909–14919.

